

# On the azimuth angle characteristics of the blast waves from an underground magazine model (IV) —Large-scale field experiments—

Yuta Sugiyama<sup>\*†</sup>, Kunihiko Wakabayashi<sup>\*</sup>, Tomoharu Matsumura<sup>\*</sup>, and Yoshio Nakayama<sup>\*</sup>

<sup>\*</sup>National Institute of Advanced Industrial Science and Technology (AIST),  
Central 5, 1-1-1 Higashi, Tsukuba-shi, Ibaraki, 305-8565 JAPAN  
Phone: +81-29-861-0552

<sup>†</sup>Corresponding author: yuta.sugiyama@aist.go.jp

Received: August 3, 2017 Accepted: February 6, 2018

## Abstract

We conducted large-scale field explosion experiments of an underground magazine model and applied an emulsion explosive of the order of kilograms. The overpressures of the blast wave were measured using piezoelectric pressure sensors. Experimental data were obtained at four azimuth angles ( $0^\circ$ ,  $60^\circ$ ,  $120^\circ$ , and  $180^\circ$ , where  $0^\circ$  defines the exit direction). As the azimuth angle increased from  $0^\circ$  to  $120^\circ$ , the peak overpressures reduced, then recovered at  $180^\circ$ . We compared the results with those of laboratory experiments using a 1-g pellet of pentaerythritol tetranitrate. The loading density, defined as the ratio of the mass of the explosive to the volume of the magazine, was equivalent in both experiments. To account for the different types of explosives, we scaled the isobaric plots of the field experiments by a conversion factor estimated from the peak overpressures of the two experiments at a reference point. For similar magazine shape and loading density, the scaled isobaric plots did not depend on the mass and the type of explosive.

**Keywords:** field experiment, blast wave, azimuth angle characteristics, underground magazine, mass and type of explosive

---

---

## 1. Introduction

An accidental explosion of high energetic materials at a magazine generates a blast wave, which can cause extensive damage and injury. The pressure increase behind it is sufficiently high to destroy a window or rupture an eardrum within a certain distance from the ignition point. In general, the extent of the physical hazard posed by the blast wave can be estimated by the value of the peak overpressure. The safety distance is known as the explosive safety quantity-distance (ESQD) and must be based on scientific evidence.

Several types of magazines are used to store high explosives. Explosions of material in an above-ground magazine with an unconfined geometry can be assumed to be like a surface explosion on the ground. Then, the isobaric lines of peak overpressure for estimating the ESQD could be described as a circle centered at the ignition point because the blast wave expands in a hemisphere. ESQD does not depend on the azimuth angle

in this case.

Unlike in a surface explosion, the blast-wave strength outside a magazine depends on azimuth angle from the exit direction. The blast wave strength decreases as the azimuth angle increases. Therefore, the ESQD from the exit could vary by azimuth angle.

For underground magazines regulated in Article 25 of the Ordinance for Enforcement of the Explosive Control Act in Japan, a protective dike must be located near the exit to minimize the damage caused by blast wave and fragments. When a protective dike is situated near the exit, reflection and diffraction at the dike disturb the blast wave from the underground magazine and changes the azimuth angle characteristics of a blast wave. Therefore, it should be understood for the development of safety regulations that take azimuth angle into account.

We previously conducted small-scale explosion (laboratory) experiments<sup>1,2)</sup> and numerical simulations<sup>3)</sup> on 1-g pellets of pentaerythritol tetranitrate (PETN). To

estimate the peak overpressure distributions for an underground magazine of arbitrary shape, we should understand how the magazine shape affects the blast wave propagation. The main parameter in the previous studies was the internal length-to-diameter ratio of the magazine,  $L/D$ . Incrementing the  $L/D$  reduced the peak overpressure and the distance between its isobaric lines and the exit. This information would be utilized to determine the ESQD. In the numerical study, the isobaric distribution was effectively described by an ellipse whose center moves with a constant velocity along  $0^\circ$  direction.

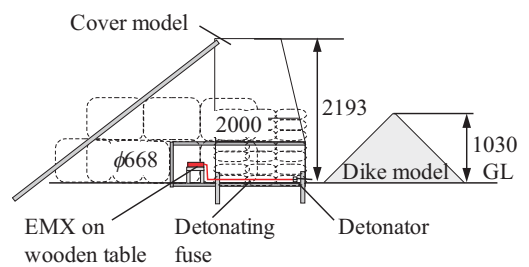
The previous papers<sup>1)-3)</sup> conducted the study of the laboratory-scale underground magazine model with a single high explosive. However, the explosive mass stored in a magazine currently being used is much larger than in laboratory experiments, and a magazine stores various type of the explosive. They may affect the proper determination of the ESQD. In the surface explosion of a single explosive, the distance of the peak overpressure distribution is scaled by the explosive mass<sup>4),5)</sup> (named the scaled distance,  $K$ ,  $\text{m kg}^{-1/3}$ ). In a magazine, there are many explosives besides PETN; well-known examples are trinitrotoluene (TNT) and cyclotrimethylene trinitramine (more commonly known as RDX). As the type of explosive changes the energy released in an explosion, an energy correction term is required when comparing peak overpressures<sup>5),6)</sup>. Many researchers define the TNT-equivalent ratio  $\epsilon$ , which denotes the released energy ratio between an explosive and TNT (used as the standard). The explosive-type effect can be quantified by the corrected scaled distance  $K\epsilon^{-1/3}$  ( $\text{m kg}^{-1/3}$ ).

In the case of the explosion inside an underground magazine, we also need to understand the mass and the type effect on the azimuth angle characteristics of the blast wave. Then, the present paper changes the mass and type of the explosive and compares the results of the field and laboratory experiments<sup>1)</sup> in the case of the explosion inside an underground magazine model.

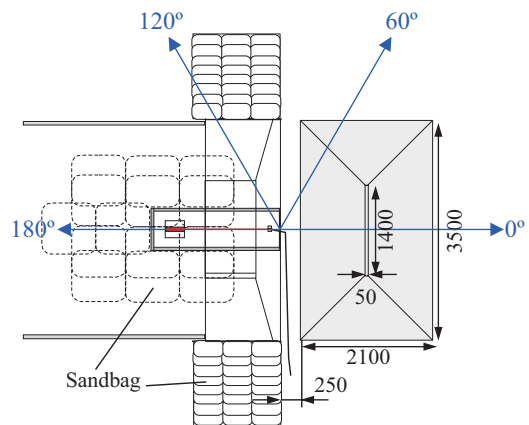
## 2. Experimental

Table 1 shows the experimental conditions, and Figure 1 shows (a) cross-sectional view with a dike, (b) top view with a dike, and (c) photograph of the underground magazine model without a dike, respectively. Article 25 of the Ordinance for Enforcement of the Explosive Control Act in Japan regulates the minimum thickness between the outer wall of the underground magazine and a free surface of the rock. In the present study, we consider it and determine the shape of the cover model as shown in

Figure 1. In Table 1, Experiments No. 1-1 to No.1-3 represent the explosion using the underground magazine model, and No. 2 denotes the surface explosion in order to discuss the azimuth angle characteristics how the blast wave from the underground magazine is enhanced and attenuated to estimate the blast wave strength of the explosive used in No. 1-1 to No.1-3. In No.1-1, a dike model is situated, whereas in No.1-2 and No.1-3, a dike model is not situated. The inner diameter  $D$  and length  $L$  of the underground magazine model are fixed at 668 mm and 2000 mm, respectively ( $L/D = 3$ ). The magazine is modeled as a cylindrical steel pipe with a wall thickness of 16 mm. The height of the cover model is 2193 mm from ground level (GL). The underground magazine model is approximately 17 times larger than the experimental model used in the laboratory<sup>1)</sup>. The loading density,



(a) Cross-sectional view



(b) Top view



(c) Photograph of the experiment without a dike model

**Figure 1** Schematics of the underground magazine model: (a) cross-sectional view, (b) top view in the case with a dike model, and (c) photograph in the case without a dike model (unit: mm).

**Table 1** Conditions of the explosion experiments.

Case	Exp. No	Dike	Mass [kg]	Density [kg m <sup>-3</sup> ]
Underground magazine	1-1	w/	5	1100
	1-2, 1-3	w/o	5	1100
Standard	2	-	10.32	1100

defined by the ratio of the mass of the explosive to the volume of the steel pipe, was almost identical in the field and laboratory experiments<sup>1)</sup> (7.13 and 7.19, respectively). Therefore, the experiments differ only by the types and masses of the explosives.

The blast wave reflections around the exit and dike model are complex. Therefore, to compare the field and laboratory experiments, we erected a solid plywood wall near the exit. In our previous experiments<sup>1)</sup>, we filled the air space inside the cover model with clay, which also suppresses the movement of the magazine model caused by the explosion. In the field experiments, we piled sandbags around the steel pipe, and omitted the cover model behind the magazine model.

Kayaku Japan Co., Ltd. supplied the emulsion explosive (EMX) in the field experiments. The EMX was coupled to a detonating fuse (Kayaku Japan Co., Ltd., 5 m, 2 lines, 10 g m<sup>-1</sup>), and exploding bridge-wire detonators RP-501 (Teledyne RISI, Inc.). The main charge was placed on a wooden table as shown in Figure 1, and the center of the main charge is adjusted at the center axis of the underground magazine model. The center of the explosive was placed 333 mm from the end wall of the steel pipe. As the masses of the explosive in the detonating fuse and the detonators summed to less than 2% of the EMX mass, we neglected the effect of the additional explosive mass, and defined the scaled distance  $K$  (m kg<sup>-1/3</sup>).

In No. 2, we conducted surface explosion experiments without any models. The explosive was placed on a wooden table with its center at 0.18 m kg<sup>-1/3</sup> above the ground.

The blast wave pressures were recorded by a digital waveform recorder (H-TECH Triple mode 30622) and piezoelectric pressure sensors (PCB 113B28, 100 mV psi<sup>-1</sup>) placed at 1 m above the ground with a 1.04 MHz sampling rate. The azimuth angles of the recordings were 0°, 60°, 120°, and 180° (see Figure 1). The ranges of scaled distances between the magazine exit and pressure sensors were  $4 \leq K \leq 25$  at 0° and  $4 \leq K \leq 16$  at 60°, 120°, and 180°. In the case without the dike, we conducted two experiments (No.1-2 and No.1-3) to check the reproducibility of the peak overpressure. The maximum deviation from the mean at each pressure sensor was within 4%, confirming the high reproducibility of the present field experiments.

### 3. Results and discussion

The left and right images in Figure 2 are high-speed photographs captured at (a) 2 ms, (b) 20 ms, and (c) 100 ms after initiation in cases (A) (with the dike) and (B) (without the dike), respectively. These images were captured with a Phantom V1210 at (1280 × 800) resolution and 12600 fps from the 90° direction (i.e., the 0° direction is to the left of the magazine exit). The flash region at 2 ms is a high-temperature fire ball. At 20 ms, and 100 ms, detonation products and dust diffuses from the exit. The behaviors of the fire ball, detonation products and dust change when the dike is installed. Specifically, the fire ball is reflected at the rising slope of the dike (see Figure 2A-a), and the

detonation products and the dust cannot diffuse along the 0° direction; instead, it rolls up around the dike. In contrast, without the dike, the fire ball, the detonation products and the dust expand smoothly from the exit along the 0° direction (Figure 2B). Similar features were observed in previous numerical visualizations<sup>3)</sup>.

The peak overpressures were obtained by interpolating the experimentally obtained pressure-time histories using smooth cubic natural spline functions. The peak overpressure distributions used in the safety analysis are displayed in Figure 3. In the no-dike case, the peak overpressures were averaged over No. 1-2 and No. 1-3. The azimuth angle characteristics in the field experiments were similar to those in the laboratory experiments<sup>1), 2)</sup>, and are elaborated below.

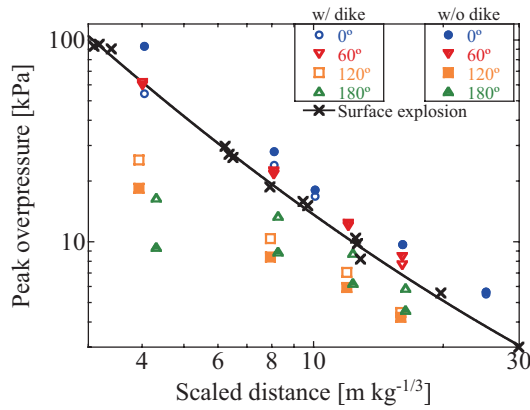
- As the azimuth angle increased from 0° to 120°, the peak overpressures reduced, then recovered at 180°. As the cover model is symmetrical (see Figure 1), the blast waves propagating around the cover model from the left, right, and upper sides meet, and the superposed blast wave is locally enhanced around 180°.
- Relative to the surface explosion, the peak overpressures of the underground magazine were intensified at 0° and 60°, and attenuated at 120° and 180°.
- The dike prevents the expansion of the blast wave along the exit direction as shown in Figure 2, and attenuates the peak overpressure near the dike at 0°. However, the attenuation effect diminishes after sufficient spreading of the blast wave.
- The blast wave at  $\theta = 120^\circ$  and  $180^\circ$  is enhanced by reflections off the dike. The reflection effect continues at large scaled distances.

Figure 4 plots the normalized peak overpressure versus the azimuth angle at  $K = 16$  in the presence and absence of the dike. The peak overpressures were normalized with respect to those at  $\theta = 0^\circ$ . For comparison, the results of laboratory experiments with different  $L/D$ s<sup>2)</sup> are also plotted (solid lines in Figure 4). The normalized peak overpressures in Figure 4 were independent of the type of explosive used in the present study.

Figure 4(b) presents previous experimental data from other reports<sup>7)-9)</sup>. The 1995 laboratory experiments<sup>7)</sup> were performed using detonators alone, in the ranges  $3 \leq L/D \leq 12$  and  $0.13 \leq A_p/A_c \leq 0.32$  (where  $A_p$  and  $A_c$  are the cross-sectional areas of the passageway and chamber, respectively. In the present study,  $A_p/A_c = 1$ ). The 1998 data<sup>8)</sup> were obtained in large-scale field experiments of Model 1 in the 1995 data using TNT. None of the above experiments included a cover model. The 2008 data<sup>9)</sup> in Figure 4(b) were obtained in large-scale field experiments using TNT with a cover soil shaped similarly to the cover model in the present study. In the ranges  $3 \leq L/D \leq 21$ , and  $0^\circ \leq \theta \leq 160^\circ$ , the azimuth angle characteristics are independent of the experimental conditions. The 1995 and 1998 data at 180° disagree with the present experimental data because the earlier experiments lacked a cover model. Therefore, when determining the ESQD, we should



**Figure 2** High-speed photographs captured at (a) 2 ms, (b) 20 ms, and (c) 100 ms after ignition in case of (A) No.1-1 (with the dike) and (B) No.1-2 (without the dike).



**Figure 3** Peak overpressure distribution. Colored and black plots denote the results of explosion inside the underground magazine (No. 1-1 to No. 1-3) and surface explosion (No. 2), respectively. The black line is fitted to the experimental data of No. 2.

carefully consider the geometrical irregularity of the explosive system.

The solid gray line in Figure 4(b) is described by the empirical equation proposed by Skjeltnorp<sup>10</sup>, who performed experiments of  $L/D = 86$ . For a reason described below at least, the azimuth angle characteristics notably differ between Skjeltnorp's and our studies. At large  $L/D$ , a fully developed one-dimensional shock wave expands from the tube exit, and linearly propagates in the  $0^\circ$  direction. The decay of the normalized peak overpressure with increasing azimuth angle is more promoted in Skjeltnorp's data than in the other data.

To discuss the effect of explosive type on ESQD, we compared the peak overpressures of surface explosions of EMX (No. 2) and a PETN pellet<sup>1</sup>. The results are shown in Figure 5. The exploding PETN pellet released more energy than the exploding EMX. The PETN equivalent ratio of EMX, denoted by  $\epsilon_{EMX}$ , was estimated by the following method.

- The 13 EMX points ( $\times$ ) in Figure 5 were shifted to the empirical curve of the PETN pellet<sup>1</sup> at constant peak

overpressures, obtaining the equivalent scaled distances  $K_{PETN-eq,i}$  (one example is described as green dashed line in Figure 5).

- The PETN equivalent ratio of the  $i$ -th point ( $\epsilon_{EMX}$ ) <sub>$i$</sub> , where  $1 \leq i \leq 13$ , was calculated by Equation (1).

$$(\epsilon_{EMX})_i = \left( \frac{K_{PETN-eq,i}}{K_{EMX,i}} \right)^3 \quad (1)$$

- The 13 values of ( $\epsilon_{EMX}$ ) <sub>$i$</sub>  were averaged to obtain the PETN equivalent ratio  $\epsilon_{EMX}$ .

In the present study,  $\epsilon_{EMX}$  was estimated as 0.60. Using these data, we will discuss the type of explosive assuming an isobaric distribution.

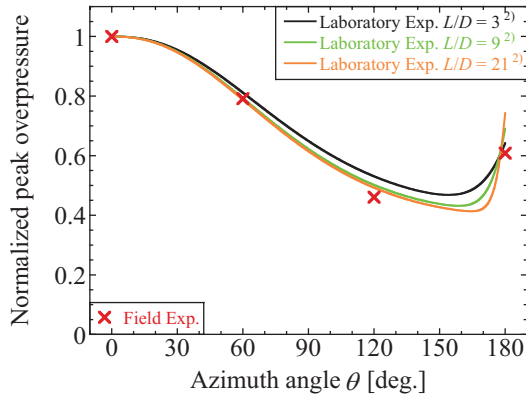
Explosions result in blast waves, ground vibrations, fragments, and debris. As the blast wave affects the widest area, the ESQD could be determined by the isobaric lines of the peak overpressure. To this end, the data acquired at  $0^\circ$ ,  $60^\circ$ ,  $120^\circ$ , and  $180^\circ$  in Figure 3 were fitted by quadratics on a log-log plot to obtain the representative curve as a function of scaled distance  $K$ . The fitting equations are given by :

$$X = \log K, \quad (2)$$

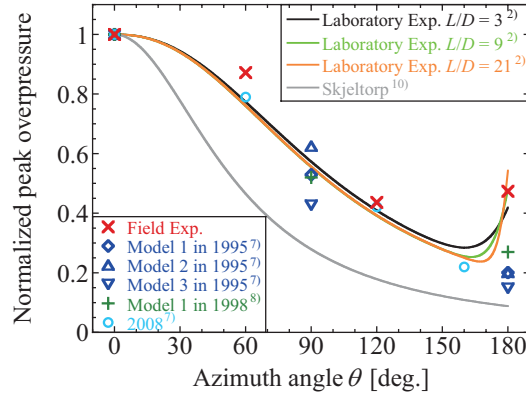
$$\log(p_{peak}) = a + bX + cX^2, \quad (3)$$

where  $a$ ,  $b$ , and  $c$  are the fitting parameters. The values of the fitting parameters are listed in Table 2. Figure 6 shows the isobaric distributions of the PETN pellet<sup>1</sup> and the EMX in cylindrical coordinates (scaled radius and azimuth angle) in the presence and absence of the dike. The origin of the coordinate system is the exit of the underground magazine. As  $\epsilon_{EMX}$  is below unity, each of the colored plots is located inside the corresponding isobaric line of the PETN pellet.

To investigate the type of explosive in Figure 6, we introduce the previous data of Kingery<sup>11</sup> and Sugiyama et al.<sup>12</sup>. They implied that the vertical axis of the peak overpressure distribution outside the underground magazine can be scaled by the peak overpressure ratio at



(a) with dike



(b) without dike

**Figure 4** Azimuth angle characteristics at  $K = 16$ . The peak overpressures are normalized by those at  $0^\circ$ .

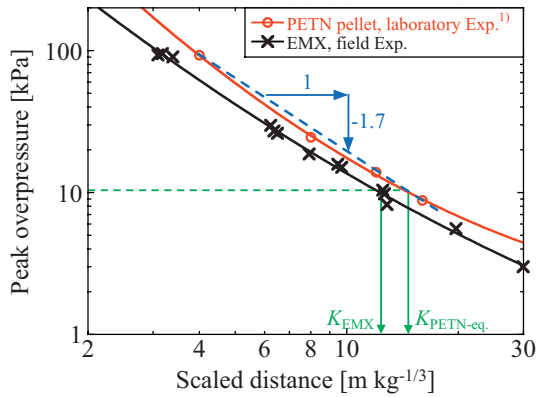


**Figure 5** Peak overpressure distributions in the surface explosion experiments.

a reference point. In the present study, we used the peak overpressures at  $K = 16$  and  $0^\circ$  as the reference data, experimentally determined as 9.70 and 12.2 kPa for the EMX and PETN pellet<sup>1)</sup>, respectively. The ratio of these peak overpressures (0.795) can scale the vertical axis of the peak overpressure distribution.

The linear attenuation ratios of the peak overpressures between 9 and 100 kPa were estimated as  $-1.70$  and  $-1.69$  for the PETN pellet and EMX respectively (see Figure 5), and were independent of the type of explosive used in the present study. Therefore, the peak overpressure ratio of 0.795 on the vertical axis corresponds to the conversion of the horizontal axis in Figure 5 multiplied by a conversion

**Table 2** Fitting parameters in Equation (3).

	$\theta$	$a$	$b$	$c$
w/ dike	$0^\circ$	2.4817	-1.2151	-0.0210
	$60^\circ$	2.6643	-1.4297	-0.0380
	$120^\circ$	2.1035	-1.1604	-0.0320
	$180^\circ$	0.5478	2.0155	-1.5112
w/o dike	$0^\circ$	3.4920	-2.8511	0.6478
	$60^\circ$	2.6396	-1.4020	-0.0156
	$120^\circ$	1.8906	-1.0662	0.0104
	$180^\circ$	0.1229	2.3188	-1.5486

factor  $C$ , where  $C = 0.795^{-\frac{1}{-1.69}} = 1.15$  for EMX. The corrected isobaric lines of the peak overpressures in cylindrical coordinates are shown in Figure 7. Here, the scaled radius of each plot is 1.15 times that of Figure 6. Our analysis properly corrects the explosive-type differences in the isobaric distribution of the peak overpressures at  $0^\circ$  and  $60^\circ$ . Because the field experiments did not include the cover model behind the underground magazine, the volumetric expansion of the blast wave was larger, which could be a reason for more reduction of the peak overpressure than that at the laboratory experiments. Therefore, the plots at  $120^\circ$  and  $180^\circ$  located inside the lines of PETN pellet<sup>1)</sup>. In a previous result<sup>2)</sup>, the azimuth angle characteristics were unchanged in the range  $3 \leq L/D \leq 21$ . In such condition, the wave strengths of blasts from different explosive types could be scaled by the conversion factor estimated from the outside reference data.

From Figure 5, the PETN equivalent ratio of EMX ( $\epsilon_{EMX}$ ) was estimated as 0.60. The scaled distance of the surface explosion was then multiplied by the PETN equivalent ratio,  $\epsilon_{EMX}^{-1/3} = 1.19$ . This correction term well agrees with the conversion factor  $C = 1.15$  for the isobaric distribution of the explosion inside the underground magazine. For the present underground magazine shape, the PETN equivalent ratio can correct the isobaric distributions of different types of explosives. Because such agreement is not guaranteed, we should mention the applicability of the PETN equivalent ratio to the corrected isobaric distribution of the underground magazine.

Explosion inside a tube is strongly related to one-dimensional shock theory in tubes<sup>12)</sup>. As the length  $L$  of the tube is increased, the expansion wave eventually meets the shock wave and the peak overpressure at the exit reduces. Assuming two-dimensional axial symmetry, Sugiyama *et al.*<sup>12)</sup> numerically simulated the explosion of 1 kg of TNT inside a tunnel. They varied the length  $L$  and diameter  $D$  of the tube, and noted that increasing  $L$  weakened the blast wave strength for the same type and mass of explosive. Therefore, the isobaric distribution should be corrected not only by the PETN equivalent ratio but also by a shape-difference coefficient. Under similar conditions of  $L/D$  and loading density, the PETN equivalent ratio would determine hydrodynamic conditions (such as the shock wave strength and position

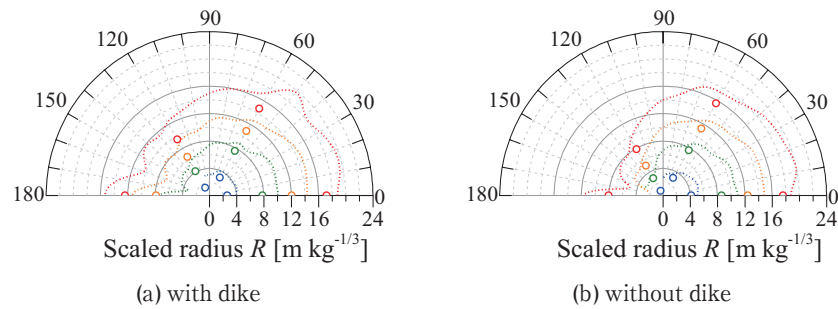


**Figure 6** Isobaric distributions of the PETNpellet<sup>1)</sup> and the EMX in cylindrical coordinates (scaled radius and azimuth angle) in case (a) with the dike and case (b) without the dike. The origin denotes the exit of the underground magazine. The blue, green, orange, and red data correspond to the peak overpressures in the surface explosion experiments of the PETN pellet<sup>1)</sup> at scale radii of 4, 8, 12, and 16, respectively. Dashed lines and plots are obtained from the laboratory experiments<sup>1)</sup> and the field experiments, respectively.

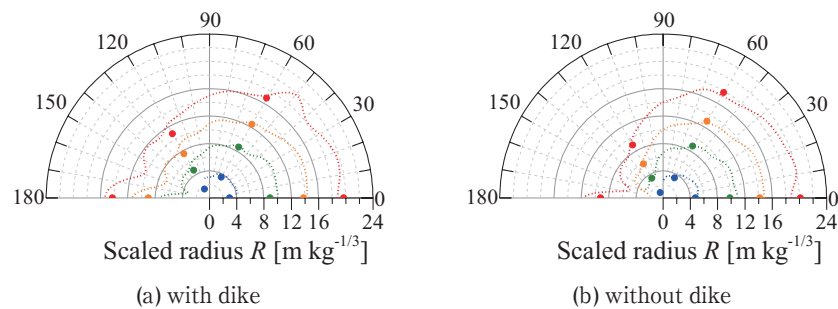


**Figure 7** Isobaric distributions corrected by the conversion factor  $C = 1.15$  in cylindrical coordinates (scaled radius and azimuth angle). Dashed lines are the same described in Figure 6, and the scaled radii of each plot are 1.15 times that of Figure 6, respectively. The blue, green, orange, and red data correspond to the peak overpressures in the surface explosion experiments of the PETN pellet<sup>1)</sup> at scale radii of 4, 8, 12, and 16, respectively.

of the expansion wave inside the underground magazine) and is then sufficient for correcting the isobaric distributions of different explosive types.

#### 4. Conclusions

We investigated a large-scale field explosion experiments of an underground magazine model and applied an emulsion explosive of the order of kilograms. The azimuth angle characteristics of the blast wave from an underground magazine model were independent of the explosive mass. The conversion factor was then estimated from the peak overpressure ratios at outside reference points. The corrected isobaric lines were independent of the explosive type.

#### Acknowledgment

This study was made possible by a METI (Ministry of Economy, Trade, and Industry) sponsored project named “Technical Standard for Explosion Mitigation of Explosives” in FY2015 and FY2016.

#### References

1) Y. Sugiyama, K. Wakabayashi, T. Matsumura, and Y. Nakayama,

- Sci. Tech. Energetic Materials, 77, 136–141 (2016).  
 2) Y. Sugiyama, K. Wakabayashi, T. Matsumura, and Y. Nakayama, Sci. Tech. Energetic Materials, 78, 117–123 (2017).  
 3) Y. Sugiyama, K. Wakabayashi, T. Matsumura, and Y. Nakayama, Sci. Tech. Energetic Materials, 78, 49–54 (2017).  
 4) C. N. Kingery and G. Bulmash, ARBRL-TR-02555, Ballistic Research Laboratory (1984).  
 5) D. L. Jones, Physics of Fluids, 13, 1398–1399 (1970).  
 6) G. F. Kinney and J.K. Graham, “Explosive Shocks in Air”, Springer, Berlin, Heidelberg (1985).  
 7) Y. Nakayama, T. Matsumura, M. Iida, and M. Yoshida, Kayaku Gakkaishi (Sci. Tech. Energetic Materials), 56, 254–261 (1995). (in Japanese).  
 8) Y. Nakayama, T. Matsumura, M. Iida, and M. Yoshida, Kayaku Gakkaishi (Sci. Tech. Energetic Materials), 59, 275–283 (1998). (in Japanese).  
 9) Y. Nakayama, D. Kim, K. Ishikawa, K. Wakabayashi, T. Matsumura, and M. Iida, Sci. Tech. Energetic Materials, 69, 123–128 (2008).  
 10) A. T. Skjeltop, R. Jenssen, and A. Rinnan, Proc. Fifth International Symposium on Military Application of Blast Simulators, 6 : 7 : 1, Stockholm (1977).  
 11) C. N. Kingery, Technical Report BRL-TR-3012 (1989).  
 12) Y. Sugiyama, K. Wakabayashi, T. Matsumura, and Y. Nakayama, Sci. Tech. Energetic Materials, 76, 14–19 (2015).